J of Nuclear Medicine Technology, first published online February 28, 2020 as doi:10.2967/jnmt.119.235960

Metastatic Prostate Adenocarcinoma with Urinary Bladder involvement by two different routes (direct extension and hematogenous seeding): Dual tracer PET (^{68}Ga-PSMA-11 and FDG) and CT Imaging features and their role in assessing and predicting response to ^{177}Lu-PSMA-617 Radioligand Therapy vis-à-vis conventional risk categories

[1,2]Aadil Adnan, [1,2]Sandip Basu

[1]Radiation Medicine Centre, Bhabha Atomic Research Centre, Tata Memorial Centre Annexe, JerbaiWadia Road, Parel, Mumbai 400012
[2]Homi Bhabha National Institute, Mumbai, India

Author for correspondence:
Sandip Basu, [1]RADIATION MEDICINE CENTRE, BHABHA ATOMIC RESEARCH CENTRE, TATA MEMORIAL HOSPITAL Annexe, JerbaiWadia Road, Parel, Mumbai, Maharashtra, India, 400 012. [2]Homi Bhabha National Institute, Mumbai, India
Phone: 91 22 24149428. Email: drsanb@yahoo.com

Keywords: Metastatic Prostate Adenocarcinoma; mCRPC;^{68}Ga-PSMA-11PET-CT; FDGPET-CT; ^{177}Lu-PSMA-617; Peptide Receptor Radioligand Therapy; Dual tracer PET-CT

Statement for any conflicts of interest: No potential conflicts of interest relevant to this article exist.

Abstract:

The present communication details on the imaging characteristics, peculiarities and response to PSMA targeted ^{177}Lu-PSMA-617 PRLT in accordance with Gleason score and use of dual tracer PET study (^{68}Ga-PSMA-11 and FDG) in patients with urinary bladder invasion/metastasis by prostate cancer, including the prognostic value of FDG-PET in predicting response to treatment. The CT attenuation units (HU) correlated with prostate primary in case of direct tumour extension from prostate, while in hematogenous metastatic seeding the HU was lower than the primary prostatic tumour. A particular point of note was that favorable outcome to ^{177}Lu-PSMA-617 PRLT was observed in patients with lesser or no baseline FDG uptake despite high Gleason score and high risk NCCN prognostic category, and did not correlate with the latter alone, while high SUVmax values on FDG PET-CT was found to be associated with adverse outcome. These findings suggested the promising role of FDG PET-CT in predicting therapeutic outcomes with more confidence, and hence the concept of dual tracer PET appeared to hold good in prostate adenocarcinoma theranostics.

Introduction:

Prostate carcinoma is the second most frequently diagnosed cancer and the sixth leading cause of cancer related death in males worldwide (1). About 20% of the patients suffer from metastatic diseases with common sites being pelvic and abdominal nodes, urinary bladder (direct infiltration >hematogeneous seeding) and skeleton (axial > appendicular skeleton) (1). On the other hand, the most common tumour involving the urinary bladder is primary urothelial carcinoma (2). Secondary urinary bladder tumours are relatively uncommon and accounts for about 2 to 13% of all tumors, majority being due to primary in prostate and adjacent organs (2, 3). Urinary bladder metastases from prostatic adenocarcinoma can occur in two ways: (i) direct extension of the prostatic tumour and (ii) multifocal, exophytic hematogeneous seeding (mimicking multifocal primary urothelial carcinoma). While the former is more common and mainly involves bladder neck and trigone, the latter is mostly multifocal and involves muscular wall more than being intravesical.

Presently the mainstay of imaging for prostate adenocarcinoma is magnetic resonance imaging (MRI)/multi-parametric MRI (mpMRI) and for urothelial carcinoma of urinary bladder, are computed tomography (CT) and MRI (4). These imaging modalities, however have limited capabilities in detecting sub-centimetric disease, particularly nodal metastases. Of late there has been remarkable improvement in molecular targeted imaging with advent of newer positron emission tomography (PET) tracers in clinical practice for prostate carcinoma. One of the most important and widely used tracers is directed towards prostate specific membrane antigen (PSMA), abundantly expressed on prostatic tumours, particularly in castration resistant cases and neovasculature of a number of solid tumours (5, 6). Targeting PSMA for imaging dates back to 2006-07, when radio-labelled J591 antibodies were used for gamma camera based planar scans (7). More recently urea based, gallium labeled small molecule inhibitors of PSMA, known as PSMA-11 or PSMA-HBED-CC is widely utilized along with other novel tracers like fluorine labeled PSMA-DCFPyL or PSMA-1007 for PET imaging and lutetium (Lu) labeled PSMA-617 for PRLT (8-12).

Herein, we present data from a series of three patients diagnosed as prostatic adenocarcinoma metastasizing to urinary bladder with different histopathological patterns and Gleason grade, treated with ^{177}Lu-PSMA-617 PRLT. The presented cases are complemented by a table (Table 1) summarizing key patient characteristics and imaging features on ^{68}Ga-PSMA-11 and flurodeoxyglucose (FDG) positron emission tomography computed tomography (PET-CT), pre- and post ^{177}Lu-PSMA-617. The primary

intent was to study the various imaging characteristics (both molecular and anatomical) of metastatic urinary bladder lesions secondary to prostatic adenocarcinoma. We have also tried to bring into attention the role of baseline FDG PET-CT study in disease prognostication and predicting long term outcome particularly after PRLT.

Case I:

A 65 years old male, known diabetic and hypertensive, on medical management, presented with lower urinary tract symptoms of 6 months duration with an episode of acute urinary retention. Further evaluation showed grade I prostatomegaly, raised serum prostate specific antigen (PSA) (58.18 ng/ml). TRUS guided biopsy showed poorly differentiated adenocarcinoma, Gleason score 4+4. Metastatic workup showed locally invasive and distant metastatic disease.He received hormonal therapy followed by bilateral orchidectomy and chemotherapy. Post-chemotherapy, presented with rising PSA with new onset left shoulder pain and was started on Abiraterone and prednisolone. Follow up showed rising PSA and disease progression and was referred for Lu-PSMA therapy. FDG PET-CT as part of pre-therapy workup showed no significant uptake in the prostatic and sacral lesions with mild to moderate hypermetabolism in the left humeral sclerotic lesion. He received one cycle of ^{177}Lu-PSMA-617. At follow up reported complete relief from shoulder pain with some reduction in PSA levels (from 65.128 to 33.062 ng/ml).

Comparative analysis of ^{68}Ga-PSMA-11 and FDGPET-CT at baseline and post first cycle of ^{177}Lu-PSMA-617 therapy is illustrated (Figure 1 and Table 1). It shows increased PSMA expression in right lobe of prostate with infiltration into urinary bladder alongwith increased PSMA expression in sclerotic lesions involving left humerus and sacrum. FDG PET-CT scan at baseline showed no significant metabolism in the prostatic lesion with low grade metabolic activity in left humeral and sacral sclerotic lesions which after first cycle of ^{177}Lu-PSMA-617therapy, demonstrated decrease in size of prostatic lesion and the intravesical component of tumour infiltration with significant reduction in PSMA expression of the lesions. No significant interval change in metabolic activity was noted in left humeral and sacral sclerotic lesions. The CT attenuation units (HU) of urinary bladder metastases showed reduction from 96 to 67 at this time, while that of prostate reduced from 100 to 70.

Case II:

The second patient was a 58 years old male patient with type 2 diabetes and hypertension, on medical management, presented with hesitancy in passing urine (in 2010). On evaluation there was raised PSA

levels; TRUS guided biopsy of prostate showing adenocarcinoma, Gleason score 4+3. MRI showed prostatic lesion with involvement of seminal vesicles and regional lymph nodes. He underwent bilateral orchiectomy. Metastatic workup was negative for metastases. Subsequently, in view of rising PSA he was started on hormonal therapy followed by Abiraterone (in view of biochemical progression). At this time, he developed metastatic liver lesions (biopsy proven) and was started on chemotherapy. Post chemotherapy there was rising PSA (153 ng/ml). He underwent channel TURP for urinary retention followed by palliative local radiotherapy (RT) to lumbar spine. Post RT, he was started on Enzalutamide, followed up with rising PSA with new skeletal lesions and was advised Mitoxantrone. Thereafter showed raised PSA (283 ng/ml) and new skeletal and hepatic lesions on FDG PET-CT. A restaging ^{68}Ga-PSMA-11 PET-CT revealed disease progression. He was referred for ^{177}Lu-PSMA-617 PRLT.

Received 5# of ^{177}Lu-PSMA-617 therapy (cumulative activity 633 mCi). Follow-up evaluations post first cycle suggested good symptomatic relief. However, no significant biochemical response was noted exceptpost second cycle, when there was some decline in PSA levels. During further follow ups, he presented with anatomical and biochemical progression (PSA 1100 ng/ml) (Figure 02). In view of disease progression, no further PRLT was planned and he was referred back to parent unit for further management. He received further hormonal therapy and multiple lines of chemotherapy with some symptomatic and biochemical response (PSA fall from maximum of 6219 ng/ml to nadir of 1761.25 ng/ml). he finally succumbed to his disease. The CT attenuation units (HU) of urinary bladder metastases reduced from 116 to 93 though the PSMA uptake increased from 27 to 36. The CT attenuation units (HU) of prostate reduced modestly from 125 to 108.

Case III:

A 65 years old male patient with no co-morbidities, presented with lower urinary tract symptoms of 8 months duration. On evaluation was found to have raised PSA (250.383 ng/ml). Further imaging with MRI revealed large enhancing lesion arising from the prostate with invasion into bladder along with multiple exophytic lesions involving right lateral and posterior walls of urinary bladder (biopsy proven to be metastatic adenocarcinoma). Digital rectal examination showed a large grade III nodular, hard prostate. TRUS guided biopsy revealed conventional prostatic adenocarcinoma, Gleason score 4+5. Metastatic workup revealed lesions suspicious for metastases. FDG PET-CT scan showed metabolically active metastatic disease. He underwent bilateral orchidectomy was started on chemotherapy with Docetaxel, which induced interstitial lung disease (reversed on steroids). Post Docetaxel follow up was

suggestive of favorable response with low S PSA, maintained for some time then presented with asymptomatic serial rise in S PSA and was put on Docetaxel re-challenge in view of biochemical (PSA 42.403 ng/ml) and morphological disease progression reflected on ^{68}Ga- PSMA-11 PET-CT scan. The patient later on took abiraterone for 3 months and was shifted to cyclophosphamide due to biochemical progression (PSA 183 ng/ml). He received cyclophosphamide for 6 months with some biochemical response (PSA 71 ng/ml) followed by biochemical disease progression (PSA 228.034 ng/ml).

The details of dual tracer PET and CT characteristics of the prostate and urinary bladder lesion has been summarized in Table 1. Interestingly, the CT attenuation units was found relatively lesser (70 vs 93) in multifocal non-contiguous bladder wall metastases (likely hematogeneous seeding) compared to that of prostate unlike in cases of direct extension of tumour into urinary bladder. On follow up, the scans for response evaluation and further treatment planning (Figure 3), on comparative analysis, demonstrated significant decrease in size and PSMA uptake in prostatic lesion with decrease in number of exophytic vesicular lesions. Significant decrease in number and PSMA uptake of abdominal and pelvic nodes with complete resolution of right hilar lymphadenopathy was noted. FDG PET-CT at this time showed complete metabolic resolution. These findings correlated well with good biochemical response (PSA 228.03 to 44.54 ng/ml).

Discussion:

Urinary bladder involvement by prostate adenocarcinoma occurs late in course of disease, thus any potential treatment is usually palliative. The symptomatic profile ranges from asymptomatic to dysuria or hematuria. It is of importance to differentiate the metastatic lesions from primary urothelial carcinomas especially in cases of multifocal bladder lesions in order to initiate appropriate therapeutic strategies early. The diagnosis is primarily by histopathology with immunohistochemistry (IHC), the latter mainly to differentiate urothelial transitional cell carcinoma (TCC) from adenocarcinoma with more confidence. The IHC markers for prostate carcinoma are prostate specific antigen (PSA), prostatic acid phosphatase (PAcP) and P504 with negative staining for P63, CK7, CK20 and villin (13). MRI forms the mainstay for imaging followed by trans-rectal ultrasound (TRUS) with limited potential of computed tomography (CT). In prostatic adenocarcinoma, ^{68}Ga-PSMA-11 PET-CT shows avid uptake at both primary and metastatic sites, which could be a valuable adjunct in making the diagnosis. Urothelial carcinoma usually shows low grade to no uptake which could be explained by scant neovascularization and associated low levels of PSMA expression as is evident from RNA-sequencing data and IHC staining (14). In the literature, couple of report exists on PSMA positivity in urothelial carcinoma (15, 16).

CT parameters, particularly, CT attenuation (HU) units can give some idea on pathological involvement of prostate. Normal prostate gland is a soft tissue structure with HU ranging from 40 to 60 in central zone and 10 to 25 HU in peripheral zone (17). Higher attenuation values of >25 HU in peripheral zone and especially equaling that of central zone is suggestive of pathological involvement, could even be malignancy (17). Prognostication in prostate carcinoma mainly depends on size of the primary tumour (T- stage), Gleason score and baseline PSA as per the NCCN and other internationally accepted guidelines and is divided into low, intermediate and high risk categories (18, 19). Avid FDG uptake on PET-CT in tumors usually reflect aggressive tumour biology and poor long-term prognosis.

In our series, two patients had direct extension of the prostatic tumour into urinary bladder involving neck and trigone, while the other had multifocal lesions involving bladder wall. One of the two patients with direct tumour extension had high risk, poorly differentiated adenocarcinoma (Case I) while the other had conventional adenocarcinoma with intermediate risk (Case II). The third patient with multifocal bladder wall lesion had high risk conventional adenocarcinoma (Case III). Case I demonstrated baseline avid PSMA and moderate FDG uptake, showed significant decline in PSA levels post ^{177}Lu-PSMA-617 therapy with partial response as per RECIST1.1 and PERCIST 1. Case II demonstrated avid PSMA and high FDG uptake at baseline scans, showed significant (> 2 folds) rise in PSA post ^{177}Lu-PSMA-617 therapy with significant disease progression culminating to death. Interestingly, in both Case I and II with direct extension of prostatic tumour into urinary bladder, the attenuation units almost corresponded with that of prostatic lesion (100 HU and 96 HU for Case I and 125 HU and 116 HU in Case II). Case III with multifocal urinary bladder wall metastases demonstrated avid PSMA with moderate FDG uptake at baseline scans, showed significant decline (> 5 folds) in PSA post ^{177}Lu-PSMA-617 therapy and partial response. CT attenuation units were less than that of prostatic lesion (93 HU and 70 HU) as against those observed in previous two cases with direct prostatic tumour extension into urinary bladder. Post ^{177}Lu-PSMA-617 therapy, all patients demonstrated significant decline in PSMA and FDG uptake in the lesions and CT attenuation units.

A point of note was that overall prognosis was found to be associated more closely with FDG metabolism rather than histopathological differentiation, Gleason score, pre-treatment prognostic category or as a matter of fact, the PSA values in the mCRPC patients. Baseline aggressive tumour biology, reflected by high SUVmax values on FDG PET-CT was found to be associated with adverse outcome, suggesting the promising role of FDG PET-CT scan in long term prognostication and predicting therapeutic outcomes, hence the concept of dual tracer PET appears to hold good in prostate adenocarcinoma.

Conclusion:

Our study illustrates that in patients of long standing metastatic prostate cancer with multifocal bladder lesions, the possibility of metastatic prostatic adenocarcinoma should be considered. Although, the definitive diagnosis is with histopathology and IHC, avid uptake on ^{68}Ga-PSMA-11 PET-CT favors prostatic origin, and could be a employed as non-invasive diagnostic adjunct to differentiate the two. CT attenuation units correlates with that of prostate in cases of direct extension of tumour into urinary bladder and is relatively lesser in multifocal bladder wall metastases (?hematogenous seeding). Hence FDG PET-CT along with ^{68}Ga-PSMA-11 PET-CT, preferably at baseline, can sub-serve prognostic and predictive implications, particularly for ^{177}Lu-PSMA-617 based PRLT. While the work bases its observations on three patients, the above interesting and intriguing observations made on this small sample size could be examined in further larger studies which would be a worthwhile exercise.

Bibliography:

1. Siddiqui E, Mumtaz FH, and Gelister J: Understanding prostate cancer. Journal of The Royal Society for the Promotion of Health 2004;124(5):219-221.
2. Melicow MM. Tumors of the urinary blad- der: a clinicopathological analysis of over 2500 specimens and biopsies. J Urol 1955;74:498-521.
3. Bates AW, Baithun SI. Secondary neoplasms of the bladder are histological mimics of nontransitional cell primary tumours: clinicopathological and histological features of 282 cases. Histopathology 2000;36:32-40.
4. Clark PE, Agarwal N, Biagioli MC, et al. Bladder cancer. J NatlComprCancNetw. 2013;11(4):446–75.
5. Chang SS, O'Keefe DS, Bacich DJ, Reuter VE, Heston WD, Gaudin PB. Prostate-specific membrane antigen is produced in tumour associated neovasculature. Clin Cancer Res. 1999;5(10):2674–81.
6. Chang SS, Reuter VE, Heston WD, Bander NH, Grauer LS, Gaudin PB. Five different anti-prostate-specific membrane antigen (PSMA) antibodies confirm PSMA expression in tumour associated neovasculature. Cancer Res. 1999;59(13):3192–8.
7. Pandit-Taskar N, O'Donoghue JA, Divgi CR, et al. Indium-111 labeled J591 anti-PSMA antibody for vascular targeted imaging in progressive solid tumors. EJNMMI Res. 2015;5:28.
8. Szabo Z, Mena E, Rowe SP, et al. Initial evaluation of [^{18}F]DCFPyL for prostate-specific membrane antigen (PSMA)-targeted PET imaging of prostate cancer. Mol Imaging Biol. 2015;17(4):565–74
9. Rowe SP, Drzezga A, Neumaier B, et al. Prostate-specific membrane antigen-targeted radiohalogenated PET and therapeutic agents for prostate cancer. J Nucl Med. 2016;57(suppl 3):90S–96S.
10. Rowe SP, Gorin MA, Salas Fragomeni RA, Drzezga A, Pomper MG. Clinical experience with ^{18}F-labeled small molecule inhibitors of prostate-specific membrane antigen. PET Clin. 2017;12(2):235–241.
11. Dietlein M, Kobe C, Kuhnert G, et al. Comparison of [^{18}F]DCFPyL and [^{68}Ga]PSMA-HBED-CC for PSMA-PET imaging in patients with relapsed prostate cancer. Mol Imaging Biol. 2015;17(4):575–84.
12. Dietlein F, Kobe C, Neubauer S, et al. PSA-stratified performance of ^{18}F- and ^{68}Ga-PSMA PET in patients with biochemical recurrence of prostate cancer. J Nucl Med. 2017;58(6):947–952.
13. Molinie V, Vieillefond A, and Michiels JF. Evaluation of p63 and p504s markers for the diagnosis of prostate cancer. Annales de Pathologie 2008;28(5):417-423.
14. Huang T, Yan Y, Liu H, et al. Metastatic prostate adenocarcinoma posing as urothelial carcinoma of the right ureter: a case report and literature review. Case Reports in Urology 2014;1-5.
15. Gupta M, Choudhury PS, Gupta G, Gandhi J. Metastasis in urothelial carcinoma mimicking prostate cancer metastasis in Ga-68 prostate-specific membrane antigen positron emission tomography-computed tomography in a case of synchronous malignancy. Indian J Nucl Med. 2016 Jul-Sep;31(3):222-4.
16. Zacho HD, Pedersen SH, Petersen A, Petersen LJ. 68Ga-PSMA PET/CT Uptake in the Ureter Caused by Ligand Expression in Urothelial Cancer. Clin Nucl Med 2019 Jul 12.
17. Dhawan S, Gothi R, Aggarwal A, Aggarwal B and Doda SS. Computed tomography in prostatic cancer. Indian J Radiol Imaging 2005;15:199-201.
18. Rodrigues G, Warde P, Pickles T, et al. Pre-treatment risk stratification of prostate cancer patients: A critical review. Can UrolAssoc J. 2012;6(2):121–127.
19. Mohler J, Bahnson RR, Boston B, et al. NCCN clinical practice guidelines in oncology: prostate cancer. J NatlComprCancNetw 2010;8:162-200.

Table1: **Summary of Histopathology, Gleason Score, NCCN Prognostic category, serum PSA level, Molecular PET (^{68}Ga-PSMA-11 and FDG) and CT imaging features at baseline and at follow-up**

	Case I		Case II		Case III	
	Baseline	Post ^{177}Lu-PSMA	Baseline	Post ^{177}Lu-PSMA	Baseline	Post ^{177}Lu-PSMA
Histopathology	Poorly differentiated adenocarcinoma		Conventional adenocarcinoma		Conventional adenocarcinoma	
Gleason Score	4+4		4+3		4+5	
NCCN Prognostic category	High risk		Intermediate risk		High risk	
PSA (ng/ml)	65.128	33.062	751	1761.25	228.03	44.54
^{68}Ga-PSMA-11 uptake (SUVmax)	64.73	28.02	27.04	36.65	116.84	83.6
FDG uptake (SUVmax)	8.38	4.41	22.88	9.63	8.4	4.5
Metastatic pattern of Urinary Bladder	Direct extension from prostate		Direct extension from prostate		Multifocal metastatic lesions involving bladder wall, ?hematogeneous	
CT attenuation units (HU) of prostate	100	70	125	108	93	67
CT attenuation units (HU) of urinary bladder metastases	96	67	116	83	70	41
Outcome	Partial Response		Progression and Death		Partial Response	

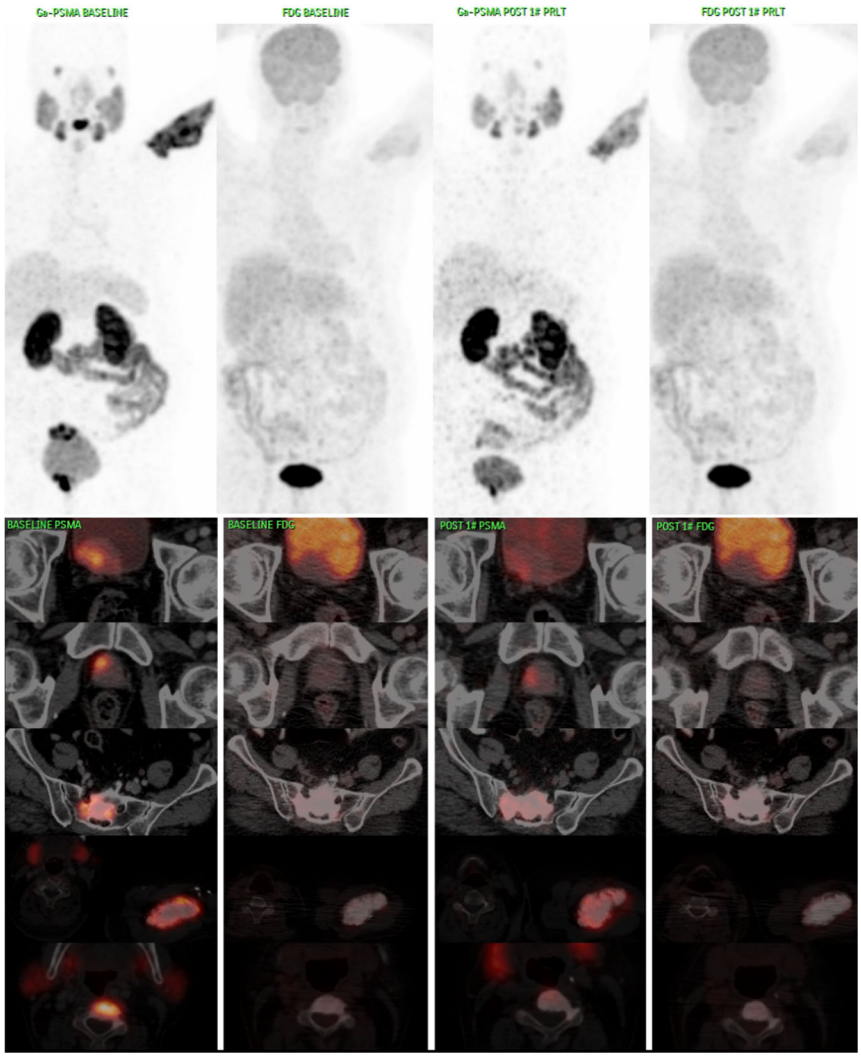

Figure 1: Comparative analysis of PSMA and FDG PET CT scans at baseline (left sided 2 panels) and post ^{177}Lu-PSMA PRLT (right sided 2 panels) of Case I.

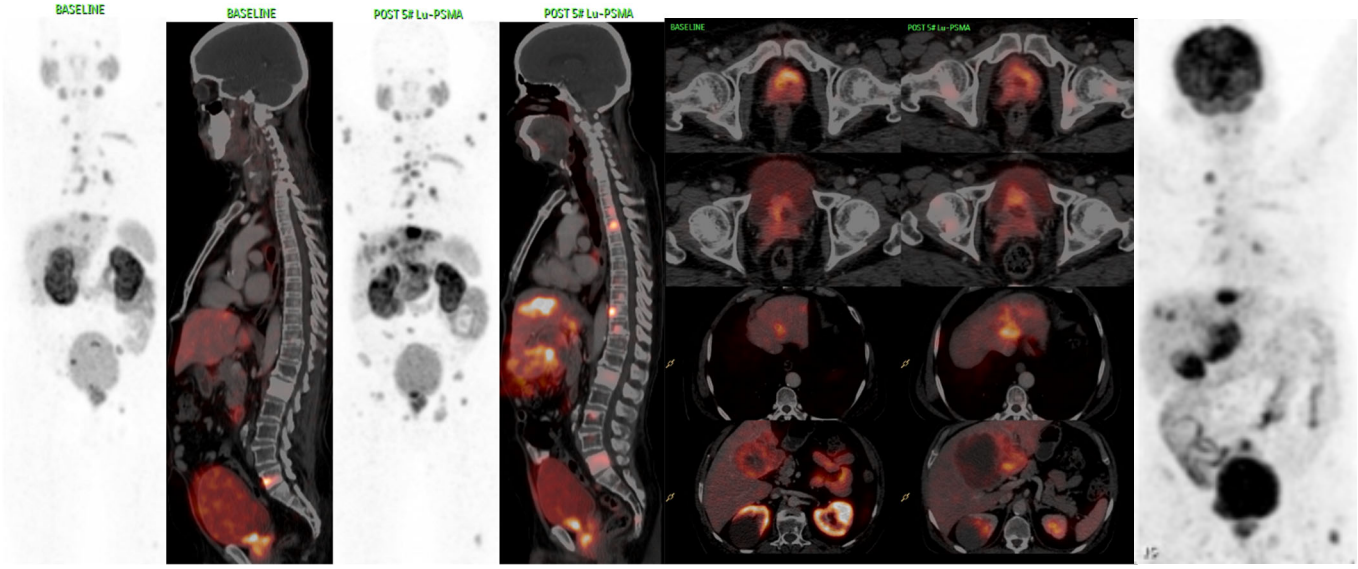

2(a) 2(a) 2(b)

Figure 2: (a) Comparative analysis of ^{68}Ga-PSMA-11 PET/CT scans at baseline and post-^{177}Lu-PSMA-617 therapy of Case II. (b) Maximum intensity projection (MIP) of baseline FDG-PET/CT scan.

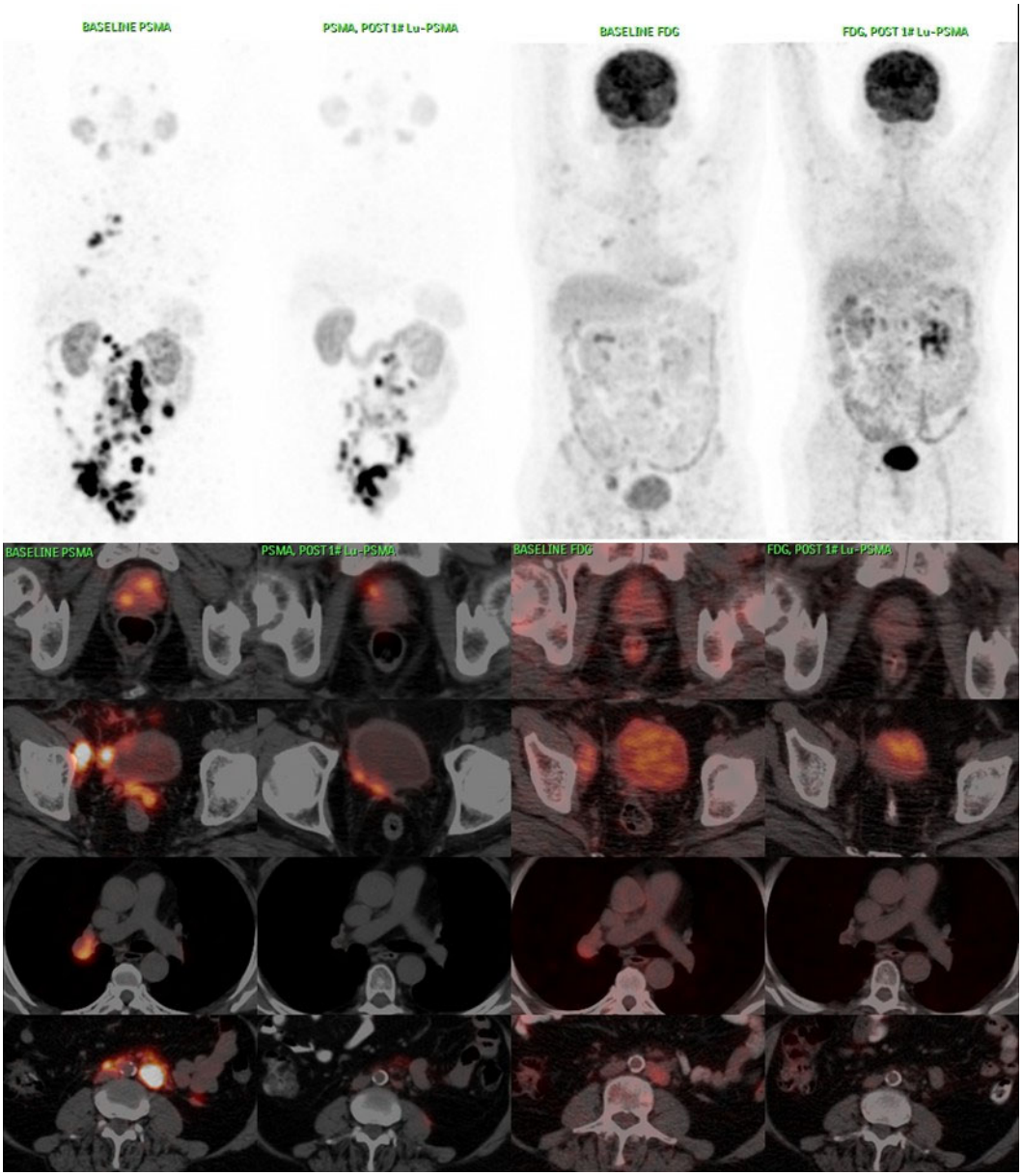

Figure 3: Comparative analysis of ^{68}Ga-PSMA-11 PET/CT (left sided 2 panels) and FDG-PET/CT (right sided 2 panels)at baseline and post ^{177}Lu-PSMA-617PRLT of Case III.